POLITECNICO
MILANO 1863

Bayesian Statistics Project : Final Report

Analyzing bayesian inference on COVID-19 infection rate

Our group :

Clément LAVAUD
clementjulien.lavaud@mail.polimi.it

Herman FORSLUND
karlherman.forslund@mail.polimi.it

Chadi KALLAS
chadi.kallas@mail.polimi.it

Hannes BACKE
hannesalfred.backe@mail.polimi.it

Marco CAYUELA
marco.cayuela@mail.polimi.it

William OLSSON
williamevert.olsson@mail.polimi.it

Academic Year 2022 - 2023

Bayesian Statistics course

I Introduction

The Covid 19 pandemic has shaken large parts of the world and has been fought using mainly various regulatory policies and vaccines. Some restricted actions, such as transferring to distance teaching, where the close contact between people may be limited, may not be as effective as restraining the night club life, where close contact may be more frequent. It is clear that many of the implemented restrictions have had a negative effect on the well-being of parts of the populations. In order to limit such negative effects, the implemented policies must be put in comparison to the restrictive element in the ordinary lives of people. This project seeks to evaluate the effectiveness of certain policies using a Bayesian modelling approach.

II Models & Methodology

II.1 Bayesian SIR Model Heuristics & Derivation

The SIR model [1], [3], [4] is a common model applied to disease spread dynamics. It is based on simple assumptions, which are stated below

1. All individuals, except a few, start out as susceptible, that is, they belong to the S group.
2. Once an individual is infected they are transferred from group S to group I via some function $\alpha(t)$ describing the transmission of infection.
3. The infected individual either survives the disease or decease due to it. Either way, the individual is transferred to the Removed group and, in the case of survival, is assumed to be immune from that point and forward. This relationship is modelled using the function $\beta(t)$ describing the rate of recovery and/or deaths.

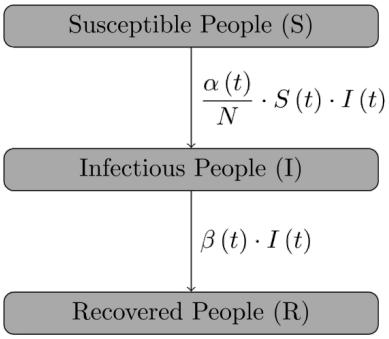

Figure 1: Continuous SIR Model

Using these assumptions, the following SIR model dynamics can to be established.

$$\begin{aligned} \frac{dS}{dt} &= -\alpha(t)\frac{I(t)S(t)}{N} \\ \frac{dI}{dt} &= \alpha(t)\frac{I(t)S(t)}{N} - \beta(t)I(t) \\ \frac{dR}{dt} &= \beta(t)I(t) \end{aligned} \tag{1}$$

This model is then discretised, yielding the following discrete stochastic model

$$\begin{cases} S_{t+1} = S_t - \Delta_t^I \\ I_{t+1} = I_t + \Delta_t^I - \Delta_t^R \\ R_{t+1} = R_t + \Delta_t^R \end{cases} \tag{2}$$

, where Δ_t^I and Δ_t^R are independent random variables incorporating/replacing the parameters $\alpha(t)$ and $\beta(t)$ in Eq. 1, with some distribution that will be modelled. Considering discrete time steps, a first attempt to

heuristically motivate their distributions would be to assume

$$\Delta_t^I \sim Bin(S_t, p^{s\to i})$$
$$\Delta_t^R \sim Bin(I_t, p^{i\to r})$$

, which can interpreted as:

- The amount of individuals going from susceptible to infected follow a binomial distribution where each individual gets infected with a probability $p^{s\to i}$. That is a simple, yet rational assumption.

To be able to utilize this model, expressions for $p^{s\to i}$ and $p^{i\to r}$ need to be given. A common way to model the transmission probability used in, for instance [6], which is also used in this model, is

$$p^{s\to i} = 1 - e^{\lambda(t)\frac{I}{P}}$$

However, due to the large population size, Δ_t^I will be close to deterministic. Hence, it is more appropriate to use another distribution in order to further increase the stochastic development of the disease. For instance, a negative binomial distribution with an alternative parameterisation could be more suitable. The same problem does not arise for Δ_t^R, due to the relatively limited amount of infected people at each time point.

If $\Delta_t^I \sim NB(\kappa, \phi)$ its mean and variance are given by

$$\mathbb{E}[\Delta_t^I] = \frac{\kappa\phi}{(1-\phi)}$$
$$\mathbb{V}[\Delta_t^I] = \frac{\kappa\phi}{(1-\phi)^2}$$

Hence, if we let $\kappa = \frac{(1-\phi)S_t p_t^{s\to i}}{\phi}$ we obtain the same mean as for the binomial distribution, i.e $S_t p_t^{s\to i}$, while the variance, $\frac{S_t p_t^{s\to i}}{(1-\phi)}$, increases with the hyperparameter $\phi \in (0, 1)$.

The main parameter of interest is $\lambda(t)$, which is aimed to describe the spreading rate. This parameter is assumed to be constant within each policy interval.

II.1.1 Setting the Priors

For simplicity, It is assumed that all the parameters are a priori independent, so that

$$\pi(\theta) = \pi(\lambda, t, p^{i\to r}) = \pi(\lambda)\pi(t)\pi(p^{i\to r})$$

Constraints on the parameters strongly influence the choice of prior distributions.

- $\lambda_i(t) \in (0, \infty)$.
- λ_i and λ_j are assumed to be independent for $i \neq j$.
- $p^{i\to r}$ is a probability, so $p^{i\to r} \in (0, 1)$.
- t must be ordered and t_i, t_j, for $i \neq j$ should be disjoint. So $t_i \in (0, T) \in \mathbb{R}$, where T is the number of days in the dataset. Hence, $t \in \mathbb{R}^{d-1}$, where d is the number of breakpoints.

In [2] a LN prior is used for λ as well as for t, but this assumes prior knowledge of the change points. Instead, assuming this information is absent and that it should be inferred, a flat prior was assigned to t.

As for λ_i, a Gamma prior was used.

$$\lambda_i \sim \Gamma(\alpha_i, \beta_i) \sim \Gamma(\alpha, \beta)$$

As opposed to [2], where the authors assumed each new policy would decrease the spread rate λ by on average 50%, here it is assumed that the policies do not have any effect on the spread rate. Hence, $\alpha_i = \alpha$ and $\beta_i = \beta$. This is mainly done in order to reduce the number of hyperparameters in the model. Using a Gamma distribution with parameters $\alpha = 2$ and $\beta = 4$ yields a similar shaped distribution as the LN distributions

used in [2], but with a thicker tail. It also has a mean in the same region as in [2]. This provides more room for λ to actually increase after a change point, while still being left-skewed. As noted later in the report, the non-effectiveness assumption for the policies does not hold, and the policies still seem to have significant impacts on the spread rate.

A suitable prior for $p^{i\to r}$ is a Beta distribution. In this case it constitutes a conjugate prior as well as satisfies the requirement $p^{i\to r} \in (0,1)$. The choice of a Beta prior hence facilitates the computations.

$$p^{i\to r} \sim Beta(a,b)$$

II.1.2 Deriving the Likelihood Function

Based on Eq. 2, $(S_t, I_t)_{t\in\mathbb{N}}$ is a markov chain. For a given parameter vector θ, it has the transition probabilities

$$q_\theta(s_t, i_t; s_{t+1}, i_{t+1}) = P_\theta(S_{t+1} = s_{t+1}, I_{t+1} = I_{t+1} = i_{t+1} | S_t = s_t, I_t = i_t) \tag{3}$$

Since Δ_t^I and Δ_t^R are independent, i.e. $P(S_{t+1}, I_{t+1}|S_t, I_t) = P(S_{t+1}|S_t, I_t)P(I_{t+1}|S_{t+1}, S_t, I_t)$, we will observe each of these factors independently.

First,

$$\begin{gathered} P(S_{t+1} = s_{t+1}|S_t, I_t) = P(S_t - S_{t+1} = S_t - s_{t+1}|S_t, I_t) = \\ P(\Delta_t^I = S_t - s_{t+1}|S_t, I_t) = \left\{\Delta_t^I \sim NB(\kappa, \phi)\right\} = \\ \frac{\Gamma(s_t - s_{t+1} + \kappa)}{(s_t - s_{t+1})!\Gamma(\kappa)}(1-\phi)^\kappa \phi^{s_t - s_{t+1}}, \end{gathered} \tag{4}$$

where $\kappa = (\frac{1}{\phi} - 1)s_t p_t^{s\to i}$, $p_t^{s\to i} = 1 - exp(-\lambda(t)\frac{I_t}{P})$ as explained before. As for the second factor, we have

$$\begin{gathered} P(I_{t+1} = i_{t+1}|S_{t+1}, S_t, I_t) = \\ P(I_t + \Delta_t^I - I_{t+1} = I_t + \Delta_t^I - i_{t+1}|S_{t+1}, S_t, I_t) = \\ P(\Delta_t^R = I_t + (S_t - S_{t+1}) - i_{t+1}|S_{t+1}, S_t, I_t) = \\ \left\{\Delta_t^R \sim Bin(I_t, p^{i\to r})\right\} = \\ \binom{i_t}{i_t + (s_t - s_{t+1}) - i_{t+1}} (p^{i\to r})^{i_t + (s_t - s_{t+1}) - i_{t+1}} \times \\ \times (1 - p^{i\to r})^{i_t - (i_t + (s_t - s_{t+1}) - i_{t+1})}. \end{gathered} \tag{5}$$

We have that Eq. (3) is simply the product of Eq. (4) and Eq. (5) which we will not write out explicitly in order to save the reader from a minor headache. Henceforth, we will use $\delta_t^s := s_t - s_{t+1}$ and $\delta_t^i := i_t - i_{t+1}$.

As for the full likelihood, we simply have that

$$\begin{gathered} P(S_0 = s_0, I_0 = i_0, ..., S_T = s_t, I_T = i_t|\theta) = \\ \prod_{t=1}^{T} P(S_t, I_t|S_{t-1}, I_{t-1}) = \prod_{t=1}^{T} P(S_t|S_{t-1}, I_{t-1})P(I_t|S_t, S_{t-1}, I_{t-1}) \end{gathered} \tag{6}$$

where $P(S_t|S_{t-1}, I_{t-1})$ and $P(I_t|S_t, S_{t-1}, I_{t-1})$ are given above. This is an even wilder expression which we will also opt to avoid writing out explicitly because of the length.

II.1.3 Conditional Distributions of Parameters

For the MCMC implementation, the interesting expressions to derive are the conditional distributions of the parameter set θ. This will only be done up to normalizing constants, because the rest is redundant for both the Gibbs and Metropolis-Hastings algorithms.

We begin by computing $\pi(p^{i\to r}|y, \lambda, t)$ since this yields a nice distribution:

$$\begin{aligned}\pi(p^{i\to r}|y,\lambda,t) &\propto \pi(y|p^{i\to r},\lambda,t)\pi(p^{i\to r}) \propto \\ \prod_{t=0}^{T-1}(p^{i\to r})^{\delta_t^i+\delta_t^s+a-1}(1-p^{i\to r})^{\delta_t^s-i_{t+1}+b-1} &= \\ (p^{i\to r})^{i_0+s_0-i_T s_T+a-1}(1-p^{i\to r})^{s_T-s_0+b-1+\sum_{t=0}^{T-1} i_{t+1}} &\\ \sim \text{Beta}(i_0+s_0-i_T-s_T+a, s_T-s_0+b+\sum_{t=0}^{T-1} i_{t+1}) &\end{aligned} \tag{7}$$

where we simply used Bayes' Theorem and the fact that most of the factors in Eq. (4) and Eq. (5) can be considered as constants when we condition on them. As for t and λ we will also only determine the posterior up to a normalizing constant, but here the expressions will not be similar to any known distribution. However, they will both be very similar because the t_i's only have direct effect on λ which in turn affects $p^{s\to i}$ which in turn affects κ. Because the utility of determining this is to provide us with acceptance probabilities, we are mainly interested in the fraction $\frac{\pi(\lambda^*|y,t,p^{i\to r})}{\pi(\lambda|y,t,p^{i\to r})}$. The posterior of t and λ (in relation to t^* and λ^*) vary with κ, and as such, the proportionality must only include the factors which include κ:

$$\begin{aligned}\pi(\lambda|t,y,p^{i\to r}) &\propto \pi(y|t,\lambda,p^{i\to r})\pi(\lambda) \propto \\ \prod_{t=1}^{T}\frac{\Gamma(\delta_t^s+\kappa)}{\Gamma(\kappa)}(1-\phi)^{\kappa}\pi(\lambda) &\end{aligned} \tag{8}$$

where $\pi(\lambda)$ is the prior given in the instructions. This yields:

$$\frac{\pi(\lambda^*|y,t,p^{i\to r})}{\pi(\lambda|y,t,p^{i\to r})} = \frac{\pi(\lambda^*)\pi(y|\lambda^*,t,p^{i\to r})}{\pi(\lambda)\pi(y|\lambda,t,p^{i\to r})} \tag{9}$$

where $\pi(y|\lambda,t,p^{i\to r})$ is provided as the product of Eq. 4 and Eq. 5. For numerical stability, we will observe the log of Eq. 9:

$$\begin{aligned}log\frac{\pi(\lambda^*)\pi(y|\lambda^*,t,p^{i\to r})}{\pi(\lambda)\pi(y|\lambda,t,p^{i\to r})} &= log(\pi(\lambda^*)) - log(\pi(\lambda)) + \\ \sum_{t=0}^{T}\Big(log(\Gamma(\delta_t^s+\kappa^*)) - log(\Gamma(\delta_t^s+\kappa)) - log(\Gamma(\kappa^*)) &\\ +log(\Gamma(\kappa)) + (\kappa^*-\kappa)log(1-\phi)\Big) &\end{aligned} \tag{10}$$

where we used properties of logarithms. The log of the prior distribution of λ_j (and consequently also λ_j^*) is simply $\propto log(\lambda_j e^{\beta_j-\lambda_j})$. The normalizing constants of $log(\pi(\lambda_j))$ are cancelled by the normalizing constants of $log(\pi(\lambda_j^*))$. Thus, they will cancel. Akin to the case of λ, we have that the posterior of t is simply described by Eq. (8), with the prior of t of course should be substituted. Identically for t, we get

$$\begin{aligned}log\frac{\pi(t^*)\pi(y|t^*,\lambda,p^{i\to r})}{\pi(t)\pi(y|t,\lambda,p^{i\to r})} &= log(\pi(t^*)) - log(\pi(t)) + \\ \sum_{t=0}^{T}\Big(log(\Gamma(\delta_t^s+\kappa^*)) - log(\Gamma(\delta_t^s+\kappa)) - log(\Gamma(\kappa^*)) &\\ +log(\Gamma(\kappa)) + (\kappa^*-\kappa)log(1-\phi)\Big) &\end{aligned} \tag{11}$$

II.2 Generalised Linear Regression Model

As observed during the pandemic, vaccination has played an important role in the spread of Covid-19. In order to incorporate the vaccination effects into the SIR model, a robust estimate for vaccination efficiency must be modelled. The efficiency of the vaccine may differ between different groups and geographical regions,

and hence a Hierarchical model is motivated. The basis of the model is simple:

$$\begin{aligned} Y_{ij} = \boldsymbol{x}_{ij}^T \beta_j + \varepsilon_{ij},\ \varepsilon_{ij} \sim \mathcal{N}(0, \sigma^2) \\ \beta_j = \theta + \gamma_j,\ \theta \sim \mathcal{N}(\mu_0, L_0) \\ \gamma_j | \Sigma \sim \mathcal{N}(0, \Sigma)\ (iid) \\ \Sigma \sim inverse - Wishart(S_0^{-1}, \eta_0) \\ \sigma^2 \sim IG(\nu_0/2, \nu_0 \times \sigma_0^2/2) \end{aligned}$$

, where Y_{ij} is the daily infection rate and $\boldsymbol{x}_j$ describes the proportion of vaccinated people.
For a more robust analysis against random effects, the analysis used data from 15 different countries, among which are Germany, Italy, Ireland, ... taken over a three months period.

II.2.1 Generalized linear model Results

First off, results for the preliminary frequentist fit can be seen in the following plot:

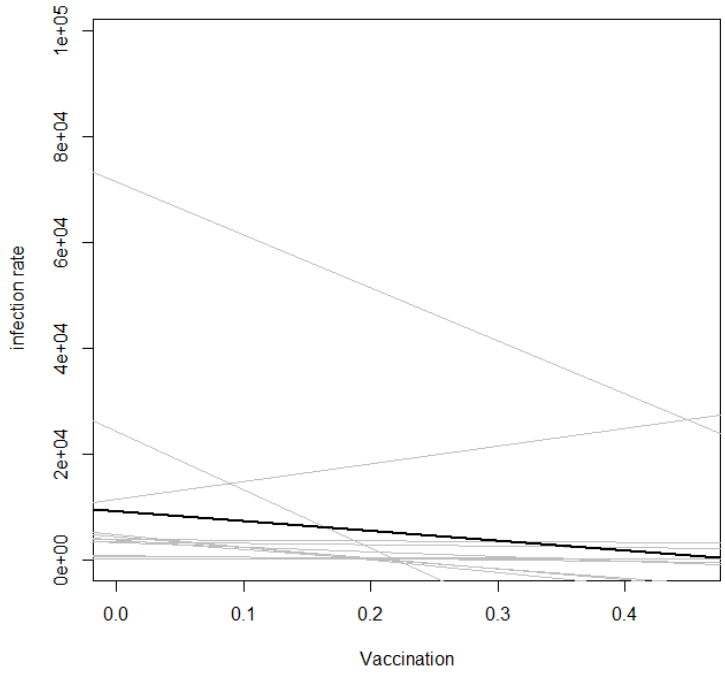

Figure 2: Frequentist Fit for the linear model: Daily infection rate vs. Vaccination percentage of the population

It's noteworthy to indicate that few countries exhibited a positive correlation between infections and vaccinations.
A gibbs Sampler was simulated for 1000 iterations, to generate 100 sample from the posterior. The initial values and priors were based on the sample parameters, namely:
- μ_0 was set as the sample fit mean.
- L_0 and S_0 was set as the sample fit variance.
The plot of bayesian posterior estimate for the infection rate versus vaccination proportion can be seen in the following:

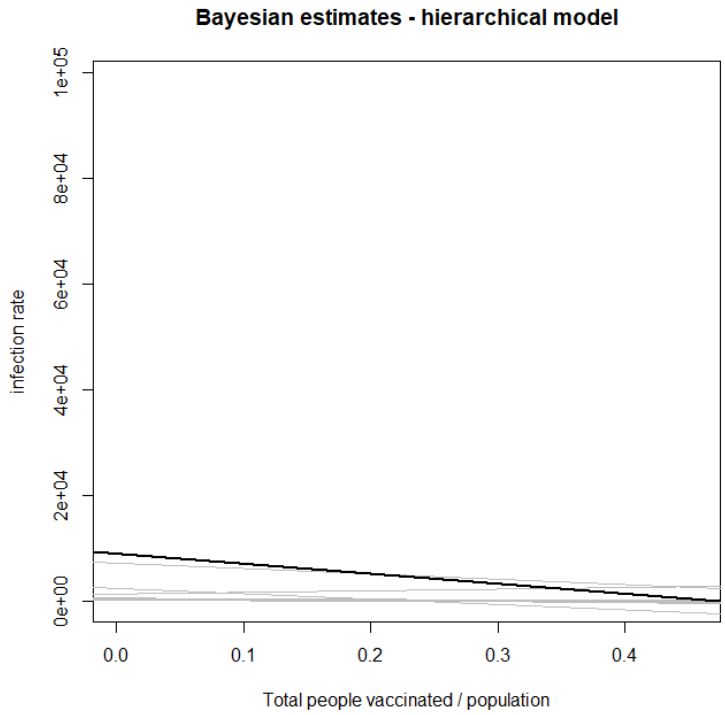

Figure 3: Bayesian Fit for the linear model: Daily infection rate vs. Vaccination percentage of the population

As seen the bayesian estimate provides a better estimation, in terms of the homogeneity of the linear model, as the lines are closer to the mean with less deviations.

Moreover it can be seen from the density plot below that the posterior density of the slope parameter is more concentrated around the mean.

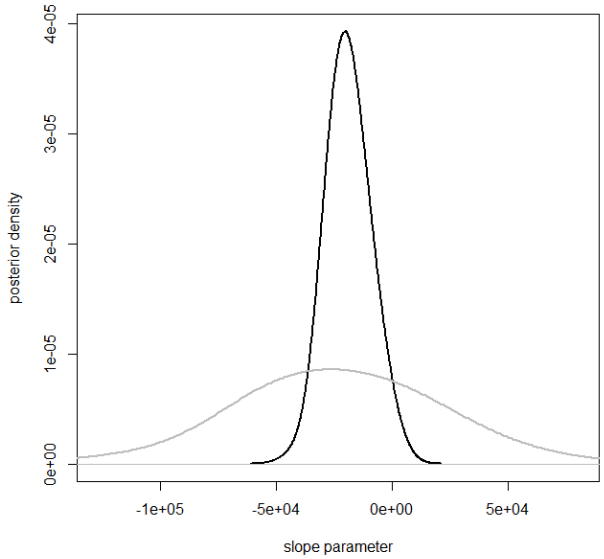

Figure 4: posterior density of the slope parameter

The mean of the slope was found to be -7907 infection per day/ proportion of population vaccinated.

III Numerical simulation

For numerical simulation a hybrid sampler was developed. In this case, it is necessary to incorporate MH steps in order to simulate the intractable full conditionals that could not be identified as any known distributions. For λ a simple symmetric proposal kernel was used, i.e $\lambda_k^* \sim \mathcal{N}(\lambda_k, \sigma^2)$, where $\sigma = 0.02$. For t another very simple proposal kernel was used, where $t_k^* \sim t_k + U\{-M, M\}$, where $M = 1$. I.e, either t increases by one time unit or it decreases by one. Since the distribution of $p^{i\to r}|y, \lambda, t$ was identified as a Beta distribution, a Gibbs step was applied to the sampling of $p^{i\to r}$.

Algorithm 1 Basic Hybrid Sampler

for $i = 1 \to N$ **do**
  draw $p_{i+1}^{i\to r} \sim Beta\left(a - s_T + s_0 - i_T + i_0, b + s_T - s_0 + \sum_{t=0}^{T-1} i_{t+1}\right)$
  for $k = 1 \to d$ **do**
    draw $\lambda_k^* \sim \mathcal{N}(\lambda_k, \sigma^2)$
    set $\alpha_k^\lambda \leftarrow \min\left\{1, \frac{\pi(y|\lambda_k^*, t, p_{i+1}^{i\to r})\pi(\lambda_k^*)}{\pi(y|\lambda_k, t, p_{i+1}^{i\to r})\pi(\lambda_k)}\right\}$
    draw $U_k^\lambda \sim U(0,1)$
    if $U_k^\lambda \leq \alpha_k^\lambda$ **then**
      set $\lambda_{k+1} \leftarrow \lambda_k^*$
    else
      set $\lambda_{k+1} \leftarrow \lambda_k$
    end if
  end for
  for $k = 1 \to d - 1$ **do**
    draw $t_k^* \sim t_k + U\{-M, M\}$
    set $\alpha_k^t \leftarrow \min\left\{1, \frac{\pi(y|\lambda_k, t_k^*, p_{i+1}^{i\to r})\pi(t_k^*)}{\pi(y|\lambda_k, t_k, p_{i+1}^{i\to r})\pi(t_k)}\right\}$
    draw $U_k^t \sim U(0,1)$
    if $U_k^t \leq \alpha_k^t$ **then**
      set $t_{k+1} \leftarrow t_k^*$
    else
      set $t_{k+1} \leftarrow t_k$
    end if
  end for
end for

As opposed to [2], our model showed unstable indications when using 3 breakpoints. Hence, it was decided to pursue the modelling using only 2 breakpoints, which provided much better consistency.

For simulation 12000 iterations were used, with a burn-in set to 2000 iterations.

III.1 Hyperparameter Dependence: A Brief Sensitivity Analysis

The SIR model used incorporates several hyperparameters, both regarding the prior distributions as well as the expressions for $p^{s\to i}$. Hence, the sensitivity of the posteriors with regards to some hyperparameters was addressed. The principle is simple: a hyperparameter is varied by using a reasonable interval, while everything else is kept constant. The posterior draws and their distributions are then plotted. Specifically, the posterior distribution of λ, $p^{i\to r}$ and t were analysed, by varying the parameters ϕ, a and b.

III.1.1 Varying ϕ

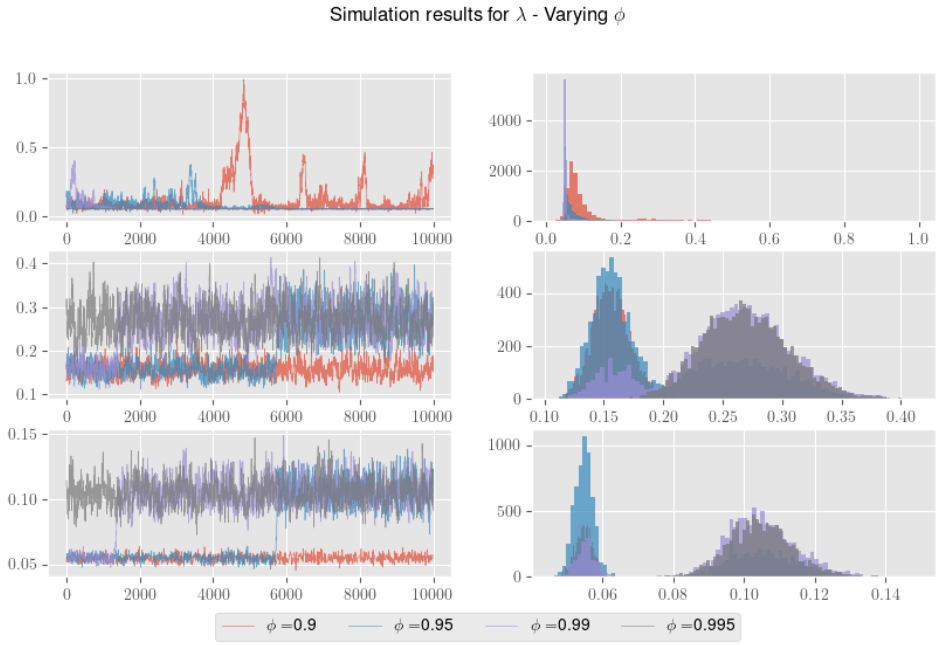

Figure 5: λ dependence on ϕ.

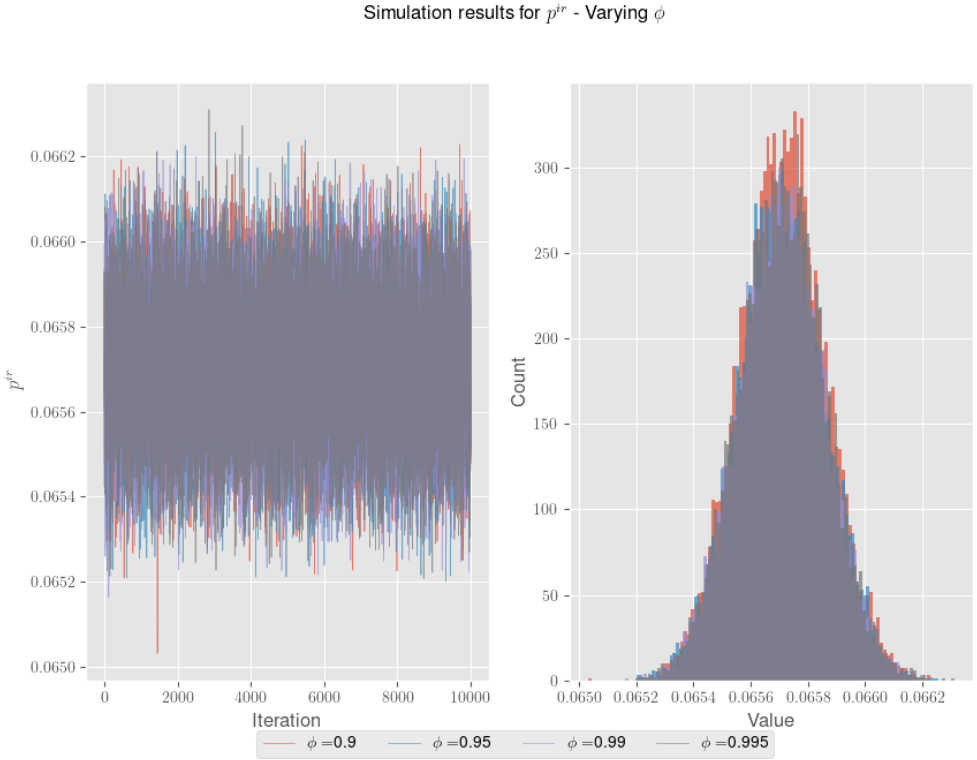

Figure 6: $p^{i \to r}$ dependence on ϕ.

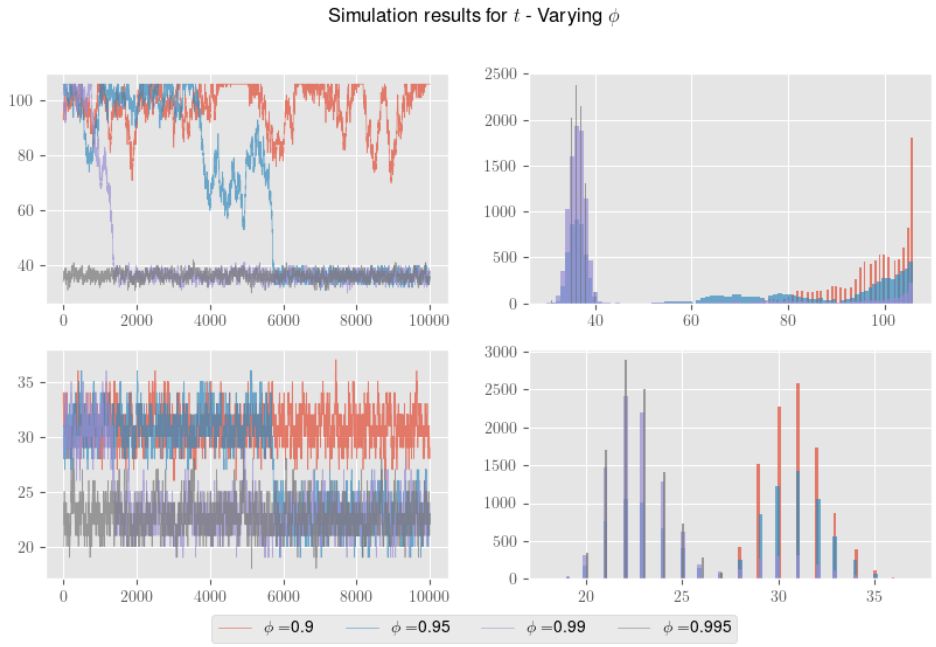

Figure 7: t dependence on ϕ.

III.1.2 Varying a

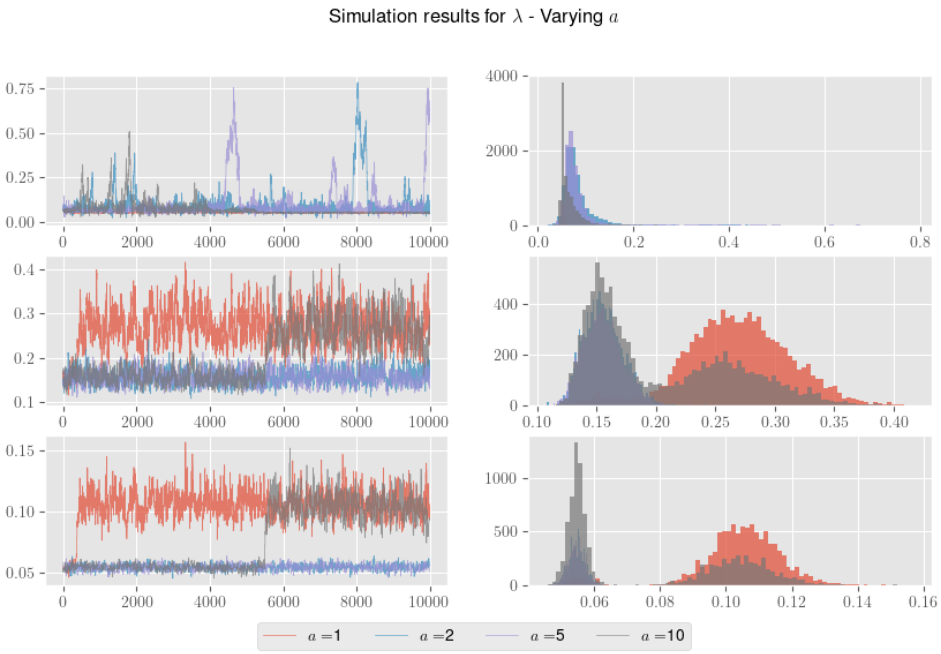

Figure 8: λ dependence on a.

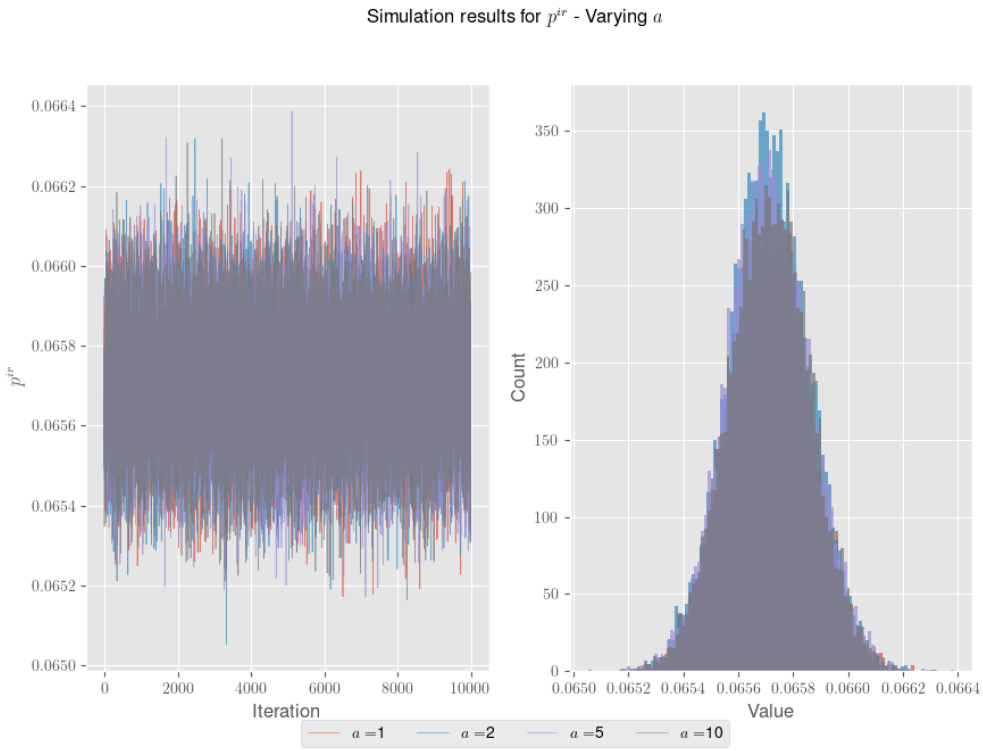

Figure 9: $p^{i \to r}$ dependence on a.

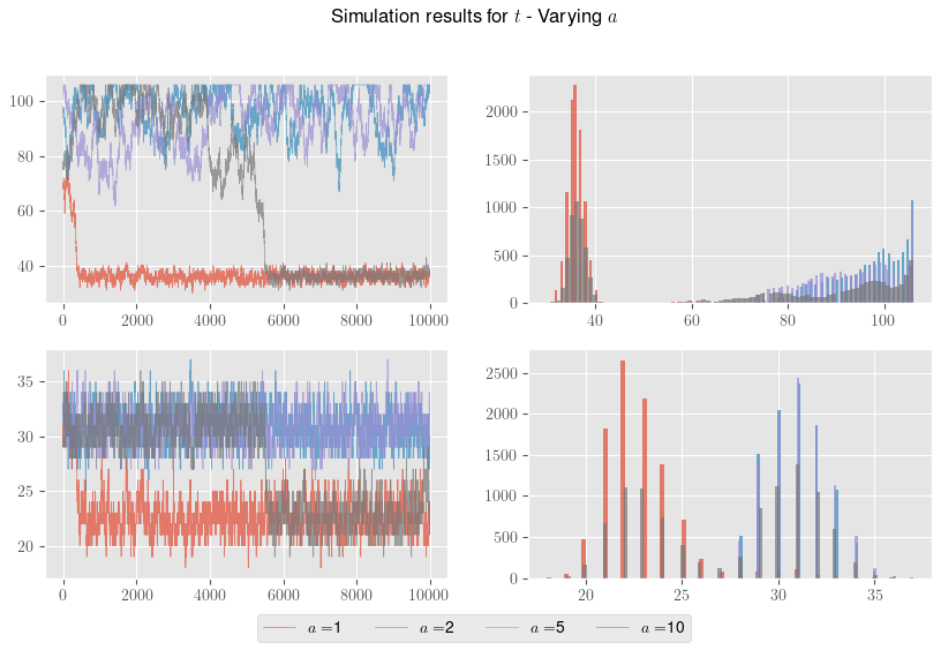

Figure 10: t dependence on a.

III.1.3 Varying b

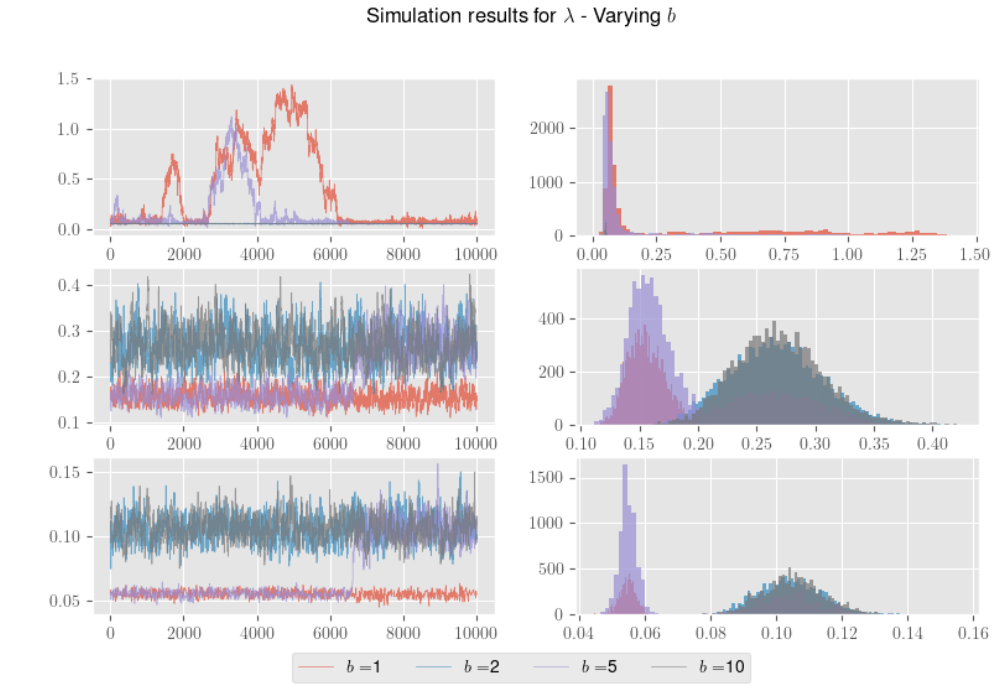

Figure 11: λ dependence on b.

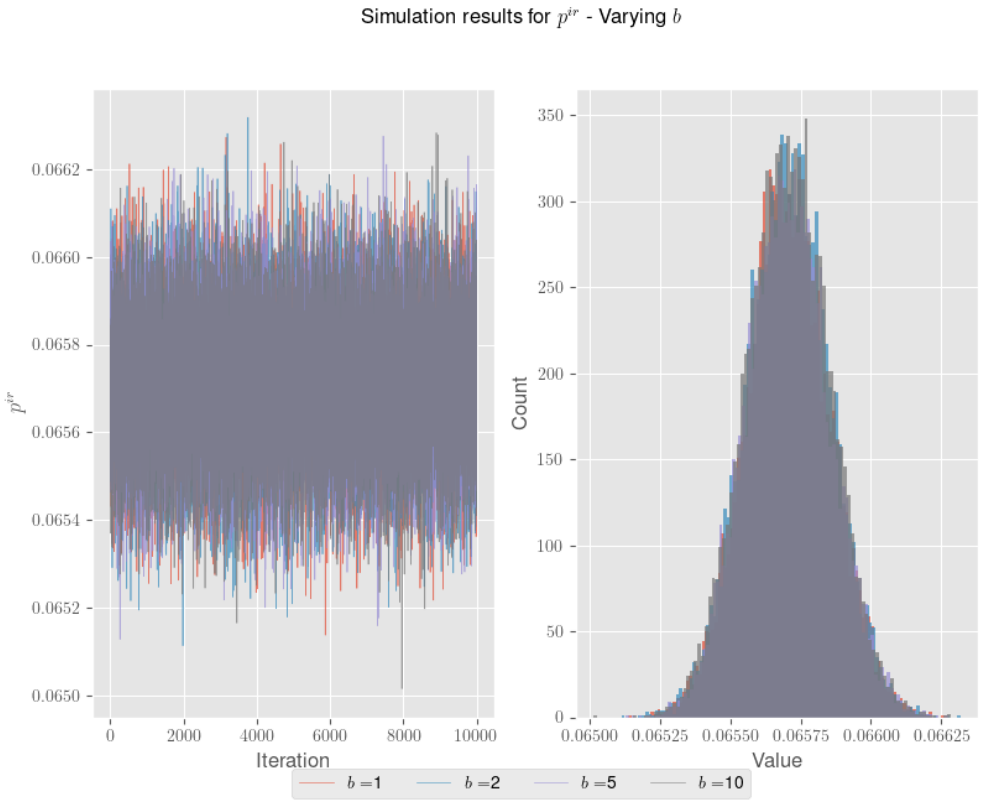

Figure 12: $p^{i\to r}$ dependence on b.

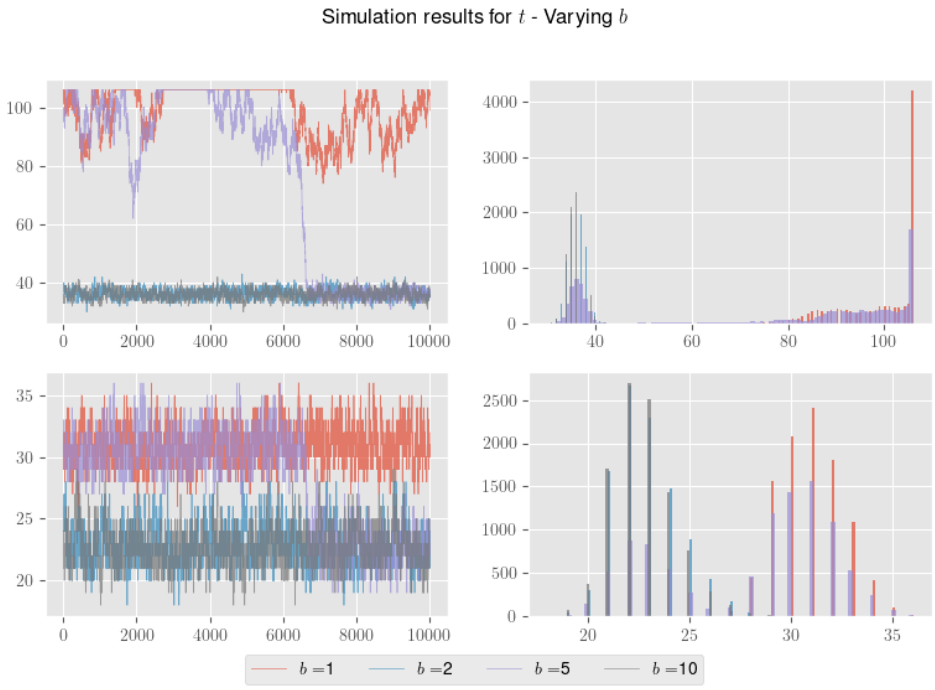

Figure 13: t dependence on b.

The first observation to make is that $p^{i\to r}$ does not seem to be sensitive to changes in the parameters ϕ, a or b. Although the expression for $\pi(p^{i\to r}|y,\lambda,t)$ contains both a and b, the effect of the relatively small values of the parameters is negligible in comparison to the other terms, i.e the terms $i_0 + s_0 - i_T - s_T$ and $s_T - s_0$.

We may also note some unstable behaviour for both λ_i and t_i when varying out hyperparameters. Such behaviour is undesirable and hence the choice of hyperparameters was partly based on the stability of the simulations. As a future improvement, these hyperparameters could be further analysed and likely be chosen more appropriately.

IV Data & Preprocessing

IV.1 Datasets

The data we used needed to fit properly with the model. Here are the datasets we had at our disposal:

- **World wide covid dataset:** this dataset contains information on new cases, hospitalisations, vaccinations, deaths linked to covid and other characteristics as GPD, population, etc... for each country in the world. These data are gathered by the World Health Organization (WHO).
- **Germany covid cases:** this dataset contains the number of new cases each day in each region of Germany according to age and sex since the start of the outbreak. [5]

IV.2 Preprocessing

All data points (from [5]) were grouped and aggregated by day. If we plot the number of cases each day in Germany we can notice that the curve is not smooth because of the delay of testing on the week-ends:

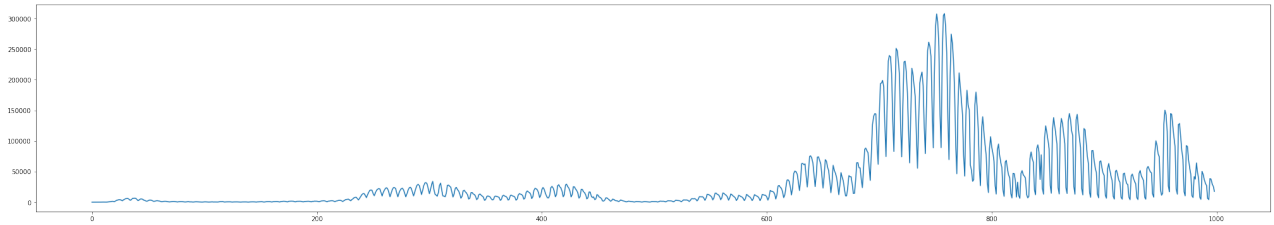

Figure 14: New cases per day in Germany

By applying a moving average with a window of 7 days to smooth the curve, we obtain the following:

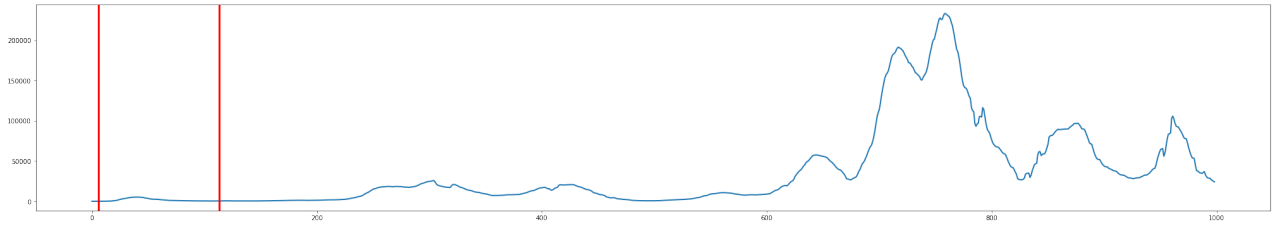

Figure 15: New cases per day in Germany (smoothed)

For the following, we kept into account the first wave of the outbreak (1st March - 15th June) which is contained in the red box in figure 9.

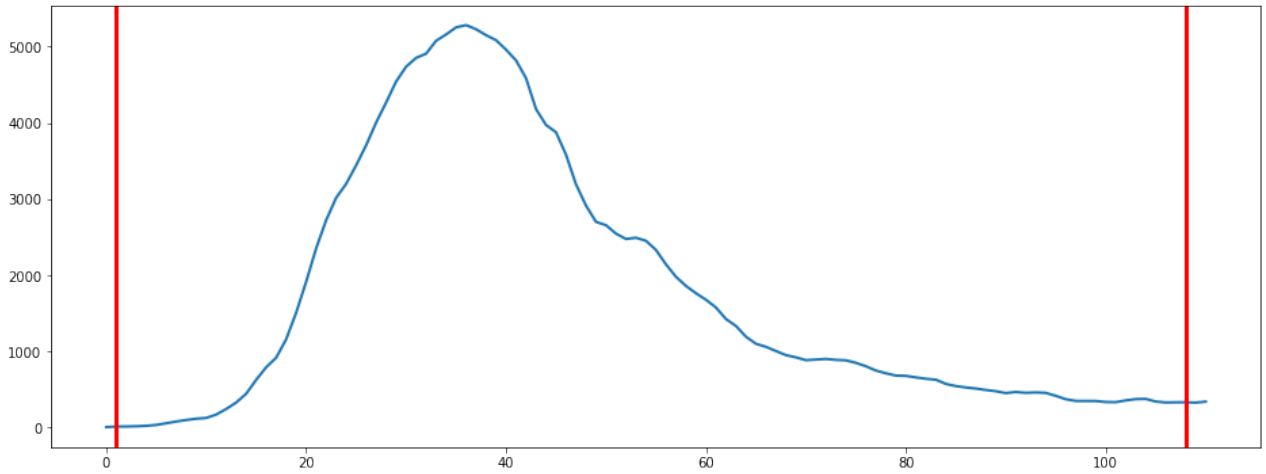

Figure 16: New cases per day in Germany (smoothed) - first wave

V Results

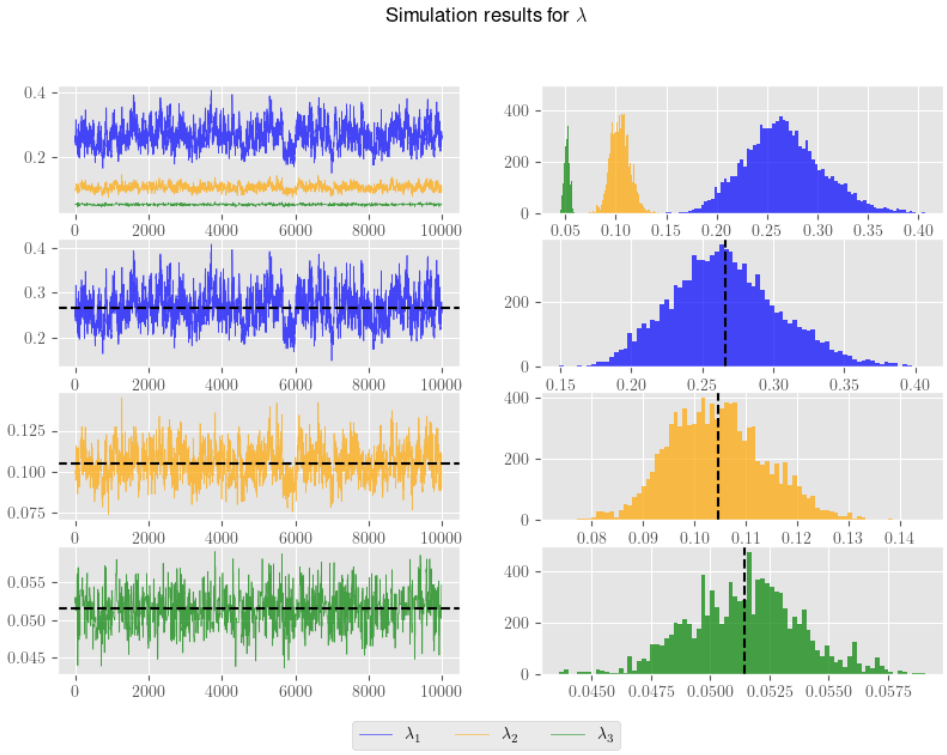

Figure 17: Simulation traceplot for λ.

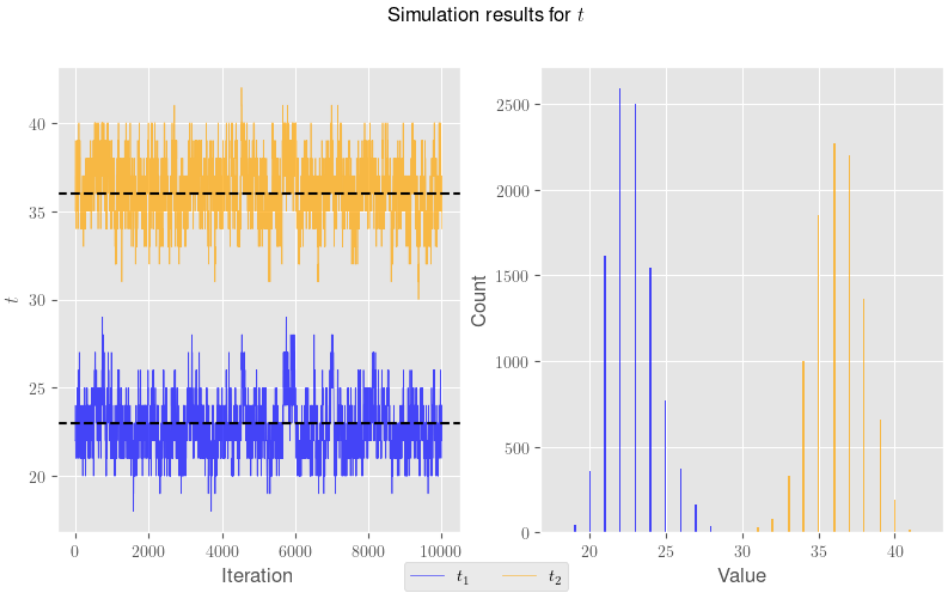

Figure 18: Simulation traceplot for t

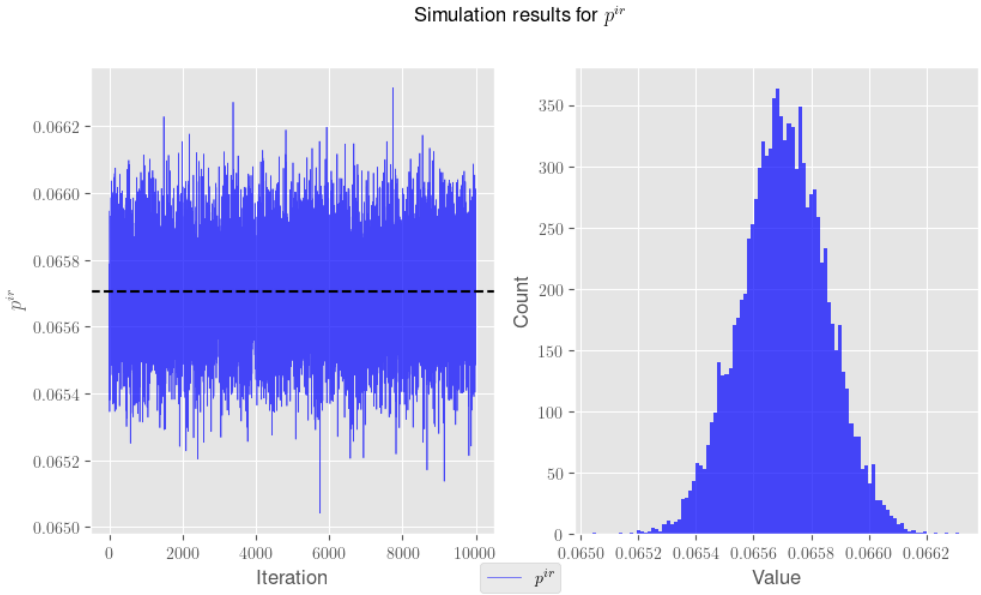

Figure 19: Simulation traceplot for $p^{i \to r}$

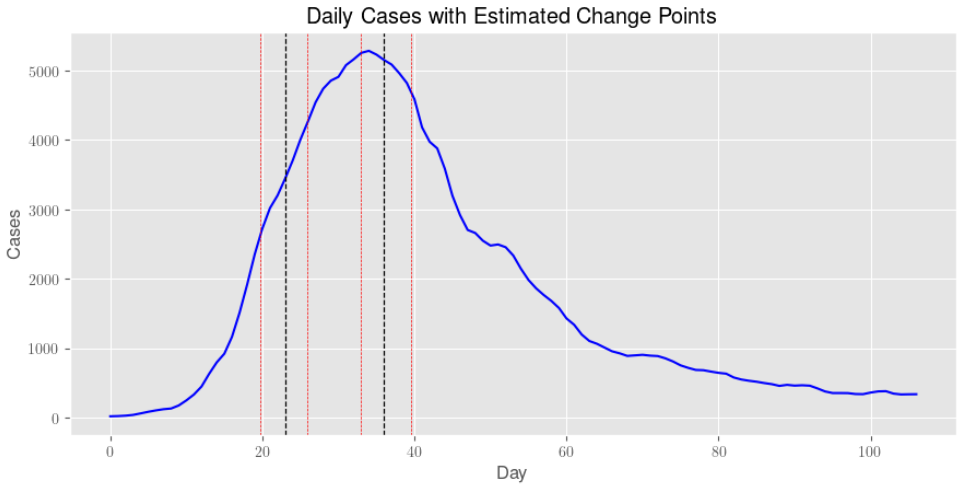

Figure 20: Change points t_1 and t_2 (black) along with the 95% HPD interval (red).

Fitting the posterior estimation to a Gaussian distribution allows for an estimate of the 95% HPD interval. The final parameter values as well as their respective HPD intervals are reported in Table 1.

Parameter	Posterior mean	95% HPD
$p^{i \to r}$	0.0657	(0.0654, 0.0660)
t_1	22.7956	(19.7426, 24.8486)
t_2	36.2461	(33.00, 39.491)
λ_1	0.2666	(0.1916, 0.3417)
λ_2	0.1046	(0.0859, 0.1233)
λ_3	0.0515	(0.0469, 0.0560)

Table 1: Final results.

VI Conclusions & Remarks

As several things differed between this project and [2], it is hard to make a direct comparison. It is however useful to briefly address the plausibility of our results and estimations. The model generally seems sound, and all our parameters have rather similar values to those obtained in [2]. We may also conclude that using our model, there seems to be quite a significant change in the spreading rate parameter λ before and after each breakpoint, even though we applied a prior with a thicker tail. A decrease in λ can be observed for each breakpoint, which also seems to coincide well with the data in Figure 20

As for $p^{i \to r}$ we obtain a rather small value. This values is very consistent with the time of recovery, which we assumed to be around 14 days.

Both the breakpoints have a rather wide HPD interval which indicates some uncertainty. However, taking the smoothing effect in the preprocessing into account, as well a probably reporting delay of 2 weeks, we would expect to observe the first two changepoints around 21 March and 1 April. Although 21 March falls within the HPD of t_1, 1 April comes just short of t_2. This may however be related to the fact that we used only two breakpoints instead of three as in [2].

VII Future Research

As future Research and contributions, one can thoroughly take advantage of the generalized linear model that analyzes the effectiveness of the vaccines, and the SIR model. A suggestion would be to set the prior for the parameter λ_i, describing the government policy regarding vaccination, dependent on the slope parameter derived from the generalized linear model.

References

[1] Linda J.S. Allen. Some discrete-time si, sir, and sis epidemic models. Mathematical Biosciences, 124(1):83–105, 1994.

[2] Jonas Dehning, Johannes Zierenberg, F. Paul Spitzner, Michael Wibral, Joao Pinheiro Neto, Michael Wilczek, and Viola Priesemann. Inferring change points in the spread of covid-19 reveals the effectiveness of interventions. Science, 369(6500):eabb9789, 2020.

[3] Giuseppe Gaeta and and. A simple SIR model with a large set of asymptomatic infectives. Mathematics in Engineering, 3(2):1–39, 2021.

[4] Chunyan Ji and Daqing Jiang. Threshold behaviour of a stochastic sir model. Applied Mathematical Modelling, 38(21):5067–5079, 2014.

[5] Kaggle. Covid-19 tracking germany. https://www.kaggle.com/datasets/headsortails/covid19-tracking-germany. Accessed: 2022-11.

[6] Carsten Kirkeby, Tariq Halasa, Maya Gussmann, Nils Toft, and Kaare Græsbøll. Methods for estimating disease transmission rates: Evaluating the precision of poisson regression and two novel methods. Scientific Reports, 7(1):9496, 2017.